INTERNATIONAL ATOMIC ENERGY AGENCY
UNITED NATIONS EDUCATIONAL, SCIENTIFIC AND CULTURAL ORGANIZATION

INTERNATIONAL CENTRE FOR THEORETICAL PHYSICS
34100 TRIESTE (ITALY) - P.O.B. 586 - MIRAMARE - STRADA COSTIERA 11 - TELEPHONES: 224281/2/3/4/5/6
CABLE: CENTRATOM - TELEX 460392-1

SMR/107 - 16

WORKSHOP ON PATTERN RECOGNITION AND ANALYSIS OF SEISMICITY

(5 - 16 December 1983)

STRUCTURE OF LITHOSPHERE INFERRED FROM SURFACE WAVES

G.F. Panza

Istituto di Geodesia e Geofisica

Università di Trieste

STRUCTURE OF LITHOSPHERE INFERRED FROM SURFACE WAVES

G. F. Panza
Istituto di Geodesia e Geofisica
Università di Trieste

1. Introduction

Since the formulation of the plate tectonics theory the Mediterranean area has been recognized as the site of the continent-continent collision between the African and Euroasiatic plates. The boundary between the two plates, as defined by the seismic activity (McKenzie, 1972), starting from the Azores triple junction, crosses North Africa and Sicily, goes through the Calabrian Arc, the Apennines, the Eastern Alps, the Dinaridies and continues along the Hellenic Arc (Fig. 1). According to the theory the results of the early stages of the collision between the margins of the African and the Euroasiatic plates are the Mediterranean Alpine chains (e. g. Channel et al., 1979; Panza et al., 1980). Presently the deformations along this belt, due to the collision, go on as documented by the observed high seismicity (e. g. Karnik, 1969).

Over the past two decades a relatively large number of long-period seismograph stations have been recording teleseismic events in the European area. Some of these stations belong to the "World-Wide Standardized Seismograph Network (WWSSN)", others have been operated temporarily by a number of institutions. In Fig. 2 a great part of sta-

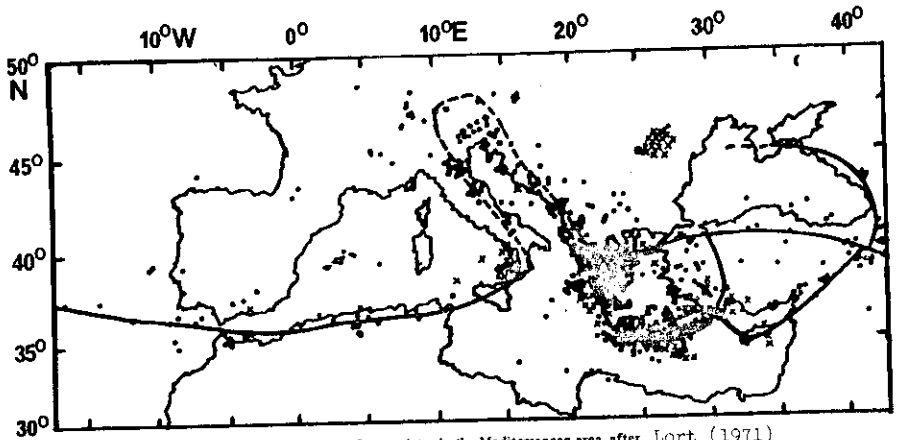

FIG. 1 - The boundary between the Eurasian and African plates in the Mediterranean area, after Lort (1971)

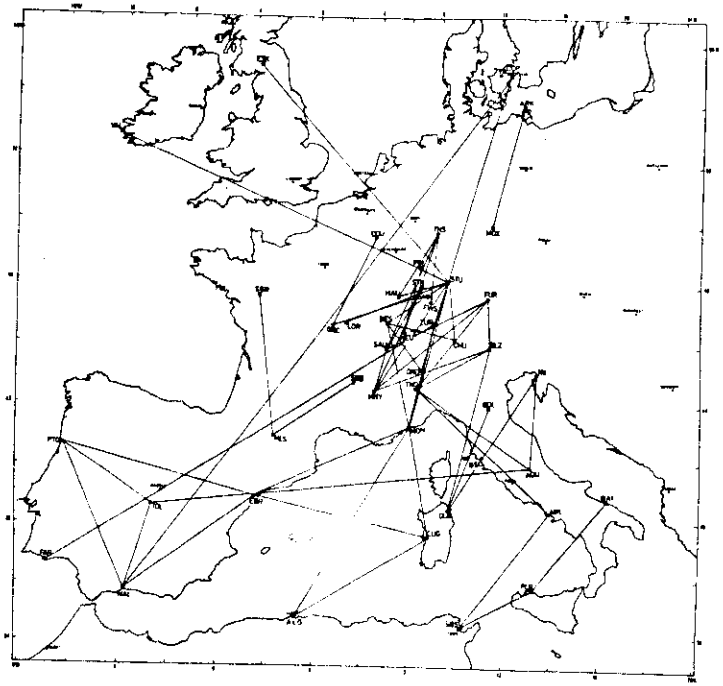

Figure 2
Long-period seismograph network and station lines used to determine 'regional' phase velocity profiles of Rayleigh waves.

tion lines, or 'profiles', are shown, along which the phase velocity of Rayleigh waves was measured.

It is seen that the region of the Western, Central and Southern Alps (Knopoff, Mueller and Pilant, 1966; Panza, Mueller and Knopoff, 1975) and the Rhinegraben (Reichenbach and Mueller, 1974; Sprecher, 1976; Seidl and Mueller, 1977) are covered by a relatively dense network of observation lines, which would allow short-period crustal studies and a detailed investigation of anisotropy as required in such complex structure. The remainder of Central and Western Europe, as well as the Western Mediterranean region, is sufficiently covered by phase velocity profiles, thus permitting a uniform inversion of the dispersion observations provided an adequate regionalization of the available phase velocity dispersion relations for seismic surface waves can be worked out.

2. Phase velocity determination

A record of the seismic waves generated by an earthquake and detected by a distant station is a function of many parameters: (a) parameters of the earthquake mechanism, e. g. depth, source orientation, initial phase, (b) elastic and anelastic properties of the medium in which the waves propagate, (c) the instrumental response that can usually be determined from the calibration pulse present on almost all long period records. The measurement of the dispersion of surface waves, which is a function of the average structure of the Earth along a given path, requires elimination of all the effects associated with the earthquake mechanism and with the instrumental response. All the following considerations can be applied to Rayleigh and Love waves.

Preliminary data analysis

The first problem which must be faced before numerical processing of seismic records is possible, is the data transformation from analog to digital form.

Selection of the digitization rate is one of the more critical decisions. The sampling rate must be at least twice the highest frequency present in the record. For long period records a digitization step of 2 sec is sufficient for the fundamental mode analysis while a Δt of 1 sec is advisable for higher mode analysis. To save computer time, before applying the Fourier transform but after filtering, data decimation can be applied . Considering the generally available equipment there are two digitization possibilities: (a) digitization at equal time increment, (b) digitization at variable time increment to sample the salient features of the record with better resolution. The first method is a little slower than the second but has the advantage that the digitized data can be immediately processed. Method (b) is faster and in some cases more accurate but requires data interpolation before any numerical processing can be performed. One easy and sufficiently accurate way of interpolating can be the Aitken-Lagrange interpolation, normally available in scientific subroutine packages. In practice the two digitization methods are equivalent and the use of one of them depends on the available equipment.

Another important point is the choice of the baseline for digitization. This line should be perpendicular to the swing of the galvanometer. Assuming that the plane of motion of the light beam is parallel to the drum axis, the baseline is determined by connecting the end of a trace on the right edge of a seismogram with the beginning of the next trace on the left edge. This is what is done in practice, but it must be pointed out that even a small deviation of the light beam plane from the

drum axis can introduce relevant errors (James and Linde, 1971). This error is frequency dependent and increases with increasing amplitude, but decreases with increasing recording speed. Since this error can generate reasonable but largely erroneous data, and thus drastically affect all inversion results, it must be recommended to all who operate a long period seismic station to determine the direction of galvanometer swing. This can be easily obtained by making a calibration pulse while the drum is stationary.

Before starting any data processing it is advisable to plot the data to detect digitization errors. Once those technical problems are solved more physical consideration must be made before starting the routine numerical processing.

In addition to dispersion, a long-period seismogram usually shows amplitude modulation or beat phenomena. Pilant and Knopoff (1964) explained this phenomenon as due to the arrival of multiple events from the same focus originating within a short interval time, or due to interference from multipath transmission. Quite often the events are neither preceded nor followed by other events within several hours, as noted from seismic bulletins, but the records show beat which then mostly are due to multipathing. If this is the case, there is practically no possibility of making use of these records, because phase velocities computed from these kinds of records show considerable scatter to the extent that their inversion gives virtually worthless results.

However not all modulations are due to multipathing. In fact from the synthetic seismograms constructed by Panza et al. (1973, 1975a, 1975b), Knopoff et al. (1973), Schwab et al. (1973) and Panza and Calcagnile (1974a, 1974b, 1975) it is quite evident that beat can be associated with source radiation. Fortunately there is a possibility of deciding

if the interference is due to the source or to multipathing. For a given azimuth, even if the modulation due to mode interference is distance dependent, salient features, like amplitude holes, are in general independent of distance. Thus the analysis of records of the same event from different stations, with approximately the same azimuth or satisfying the symmetry relations

$$\begin{gathered} |U_r^{DC}(\theta + \pi)| = |U_r^{DC}(\theta)| \\ \arg [e^{ik_j r} U_r^{DC}(\theta + \pi)] + \arg [e^{ik_j r} U_r^{DC}(\theta)] = -\frac{\pi}{2} \\ U_r^{DC}(\theta) = U_r^{DC}(\pi - \theta), \end{gathered} \qquad (1)$$

where U_r^{DC} is the Fourier time transform of the surface wave displacement at the free surface for the j-th mode, θ is the station azimuth with respect to the source line, k_j is the wave number and r is the source-receiver distance, can be used to identify multipathing.

Once this problem is solved the proper data processing for phase and/or group velocities determination can start. The most important problem is to separate the different modes excited by the earthquakes. Some synthetic seismograms containing large amplitudes of higher modes can be found in Calcagnile and Panza (1974) and Schwab et al. (1973). The problem of mode separation can be divided in two parts: (a) separation of fundamental mode from higher modes; (b) separation of different higher modes.

The isolation of the fundamental mode can be in general performed using time variable filters and time (or group velocity) windows because of the significant difference in group velocity between fundamental and higher modes. This is always true for Rayleigh waves which have travelled at least 1.000 km, while it is not generally valid for

Love waves crossing oceanic structures, because of the similarity in group velocities of fundamental and first higher mode.

Pilant and Knopoff (1964) and Knopoff et al. (1966) applied a time-variable filter to extract the fundamental mode and to improve the signal-to-noise ratio. This technique is now quite widely applied and allows to obtain dispersion data over a wide period range (20-400 sec) (e. g. Biswas, 1971).

The separation of higher modes requires a different data processing because of the similarities of the group velocities of the different modes (e. g. see Calcagnile and Panza, 1974).

Higher modes separation has been treated by Nolet (1975, 1977) and Nolet and Panza (1976).

Data processing for phase velocity determination

Once all the preliminary operations described in the previous section are completed, the basic data processing can start. The first operation is to remove the average and the linear trend from the digitized data.

Once this operation is done a set of partly overlapping band pass filters, with different central frequency, and width, is applied to the digitized record (Ormsby, 1961). A detailed description of these filters is given by Landisman et al.(1969); here it is sufficient to mention that the number of filter weights in routine work is normally taken equal to 100 for a sampling rate of 2 sec. Special situations can suggest a different choice; programs generally in use do not exceed the value of 200. In general it may be necessary to use 20-25 pass-bands of varying width to process data over the period range 20-400 sec.

In order to reject signals with a different group travel time (usually higher modes or late arrivals) as well as to isolate the Love-wave portions from those of Rayleigh waves, a sinusoidal tapered window is generally applied to all the filtered data in time domain. The center of the window is set to correspond to the group arrival time of the desired signal. In general the center of this window can be empirically determined by inspection of the filtered record. Few seconds of error in centering the window do not affect the results significantly. In some cases, and especially at long periods, instead of the tapered window it is possible to use boxcar windows. The use of a boxcar window, when possible, must be preferred because it does not introduce any distortion either in amplitudes or phases (see Fig. 3a). The limit of applicability of the boxcar window is determined by the necessity of avoiding sharp discontinuities in the time series which will generate spectral components not present in the original seismogram. In Fig. 3b, c an example is given which may be used as a guide in the choice between tapered and boxcar windows. Namely it is practically impossible to separate the two wave trains visible in Fig. 3b using a boxcar window, because it would introduce too sharp a transition between zero line and signal, generating undesirable spectral components; thus in order to reduce the contribution of the early wave train a tapered window is necessary. In the example shown in Fig. 3c, on the other side, between the two wave trains there is a portion of the signal roughly corresponding to the zero line; in this case the boxcar window must be preferred since it is possible to obtain a fairly smooth transition from zero line to signal.

To obtain a reasonable density of phase velocity points at long periods, all record lengths can be adjusted to a fixed value, say 2.500 sec, by adding, where necessary, zeros at the end of the filtered

and windowed data. Then, for each pass-band, this data set is Fourier analyzed to obtain the phase spectrum.

The method of harmonic analysis is described in several text-books. However it is worthwhile to note that for the described data processing the application of the fast Fourier transform (FFT) is not advisable since it extends the analysis over the entire spectral

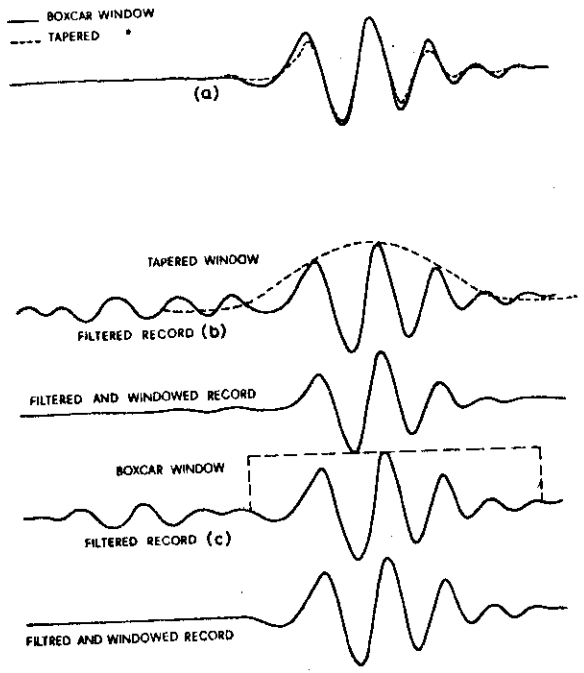

Fig. 3

Example showing the applicability of the boxcar window and the distortion introduced by tapered windows. In case (b) boxcar window can not be applied because it will generate spurius spectral components.

range. In fact for each pass band filter applied, the interest is centered in a small portion of the frequency range. For this reason it is advisable to separate the data into even and odd portions, to compute a table of sines and to use a table lookup method (Hildebrand, 1956). The procedure can be made very fast by coding the central loops in assembler language.

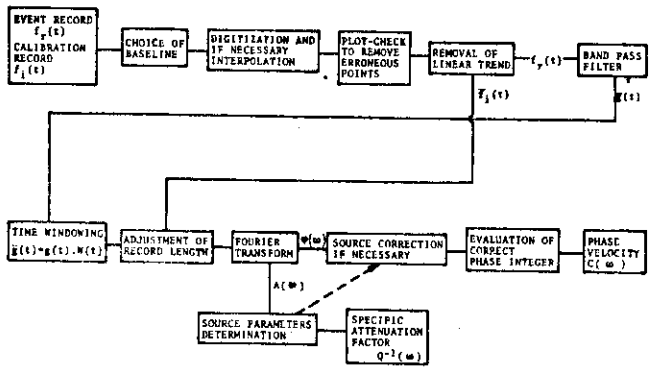

Fig. 4

Block diagram of the data processing

As mentioned before the data must be corrected for instrument response. To do this it is sufficient to digitize the calibrating pulse, usually present in all long period records, to remove the linear trend, as described before, and to Fourier analyze it. The phases so obtained are the corrections to be applied to the phases of the record.

A block diagram of the method described is given in Fig. 4.

Once the phases of a given signal in one station are obtained the phase velocity could be determined from the equation:

$$C(\omega) = \frac{\Delta}{T[N - \varphi_R(\omega) + \varphi_0(\omega)]}, \qquad (2)$$

where Δ is the distance from source to receiver in km, T is the period ($T = 2\pi / \omega$) in sec, $\varphi_R(\omega)$ is the signal phase spectrum in circles, and $\varphi_0(\omega)$ is the source initial phase in circles. However in equation (2) the quantity $\varphi_0(\omega)$ is unknown unless the source mechanism is determined. This basic problem has prevented a wider application of one station method, which would be excellent for crustal studies using near events, where geologic structure does not change markedly over the path from earthquake. On the other side, if two stations properly located with respect to the epicenter are used, then it is possible to determine the phase velocity of the waves travelling between the two stations without knowing $\varphi_0(\omega)$. In fact, if the two receivers lie on the same great circle passing through the epicentre, the source initial phase is the same at both stations (e. g. see Panza et al. 1973). Thus, using two stations, the phase velocity can be determined from

$$C(\omega) = \frac{\Delta}{T[N - \varphi_{R2}(\omega) + \varphi_{R1}(\omega)]}, \qquad (3)$$

where indexes 1 and 2 correspond respectively to the farther and nearer station. In equations (2) and (3) N is an arbitrary integer and this ambiguity produces a family of phase velocity curves consistent with the data. The proper N can easily be determined comparing the results with some standard dispersion curve (e. g. Anderson, 1964); Anderson and Harkrider (1968).

In practice the alignment condition of two recording stations is never satisfied and in general deviations of $\pm$ 5° from the great circle path are considered satisfactory. However, it must be pointed out that, in some cases, such deviation can be fairly important; namely for mechanisms having an initial phase continuously varying with θ (Panza et al. 1975a, 1975b) a 5° difference can be critical. Discontinuous variations of phases are not critical since they are always associated with zero amplitudes (Panza et al., 1973). It must be noted that a deviation of more than $\pm$ 5° from the great circle path is, in addition, not acceptable because of the lateral heterogeneities present in the Earth crust and upper mantle.

Following the ideas discussed here a large amount of phase velocity measurements have been performed by several researchers; among them can be quoted Satô (1955, 1956), Toksöz and Ben-Menahem (1963), McEvilly (1964), Toksöz and Anderson (1966), Knopoff et al. (1966), Berry and Knopoff (1967), Biswas (1971), Knopoff (1972).

More recently one station measurements have been successfully applied over large homogeneous regions to obtain phase velocities for very long periods (up to 400 sec) and for small distances in fairly homogeneous regions.

As mentioned before the use of one station requires the knowledge of the focal mechanisms. Nowadays the distribution of seismic stations is sufficient to determine focal mechanism of large earthquakes using P and S waves and computer programs are available for the estimation of $\varphi_0(\omega)$ for a given mechanism. It is more difficult to use P and S waves to determine the mechanism of small shocks because the station density is not sufficient in this case. An alternative method for mechanism determination is the use of amplitude spectra of Love or Rayleigh waves (Tsai and Aki, 1970, 1971; Aki, 1972 and Panza, 1974).

A detailed description of other methods useful in numerical analysis of dispersed seismic waves is given by Dziewonski and Hales (1972), and a comparison of different methods for surface-wave dispersion studies is given by Knopoff (1972).

3. Regionalization

In Europe it is obviously difficult to obtain dispersion profiles over tectonically homogeneous areas. For this reason a new method has been developed which allows the regionalization of experimental dispersion relations for seismic surface waves. The method consists of constructing in a trial-and-error fashion on a map iso-phase velocity lines ('isotaches') for selected periods (Fig. 5 and 6) in such a way that for each profile the following relation is satisfied:

$$\left| c_j(T_k) - \frac{\Delta_j}{\sum_{i=1}^{n} \frac{\Delta_{ji}}{c_i(T_k)}} \right| \leq \varepsilon \qquad (4)$$

where $c_j(T_k)$ is the experimental phase velocity for the period T_k, Δ_j is the total length of the profile, Δ_{ji} is the length of each segment of the j-th profile with constant phase velocity $c_i(T_k)$. n is the variable number of segments into which each profile can be divided by the given isoline set, ε is the experimental error associated with the phase velocity determination. The set of periods, T_k,

for which the isoline maps are constructed is chosen on the basis of variational parameters, computed for a three-layer upper mantle model consisting of crust, lower lithosphere and asthenosphere.

'Regional' dispersion relations can be derived by a direct comparison of these isoline maps with a tectonic map using surface features as a guideline to delineate 'homogeneous' profiles. For the European area the phase velocity lines constructed in this way can be grouped into two families according to their shape: one with an almost linear trend in the period range from 25 to 150 sec; the other with a relatively flat portion in the period range from 50 to 80 sec. To the first family belong continental rifts, orogens and marginal seas, to the second category massifs, platforms and foredeeps.

4. Inversion

A more quantitative definition of the different properties of the investigated area can only be obtained through a complete inversion of the observational data. The method of inversion used here is commonly known as the 'hedgehog' method (Keilis-Borok and Yanovskaya, 1967) and is described in detail by Biswas and Knopoff (1974). We have used as general selection criteria in the inversion the error parameters ε = 0.05 km/sec, ε = 0.08 km/sec for the longest period, and σ = 0.03 km/sec: that is, if the difference between computed and observed phase velocities exceeds ε at any individual period, or if the r.m.s. difference between the observations and the computations for the parameterized structure is greater than σ , the model is rejected. The values of ε and σ are consistent with the precision in the data sets constructed from maps of the kind shown in Figs. 5 and 6.

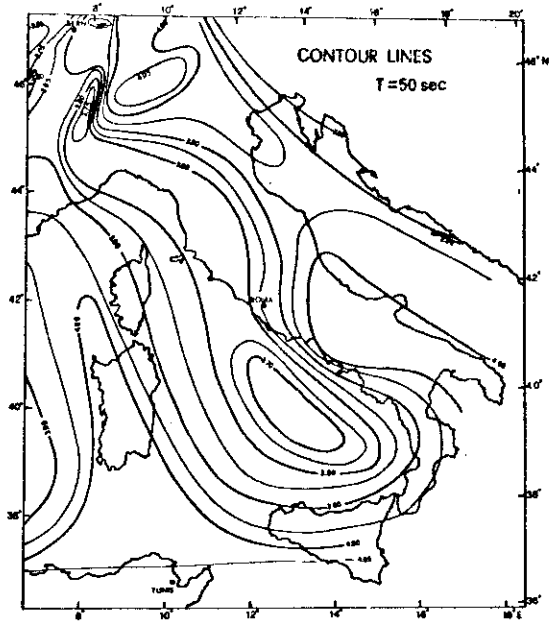

Figure 5
Isotaches at 50 sec.

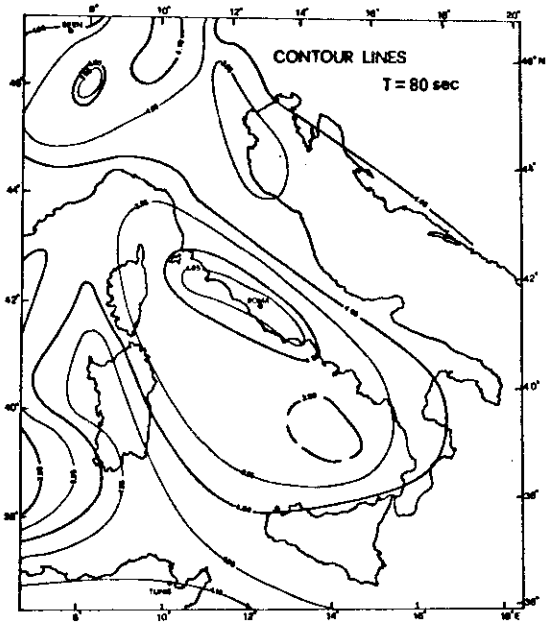

Figure 6
Isotaches at 80 sec.

In the inversion the crustal thickness for each region has been fixed in agreement with the available DSS data. The number N of layers parameterizing the crust depends upon the amount and quality of available data. The details of the different crustal models are suggested by results of DSS and indirectly relevant data (Morelli et al., 1969, 1975, 1976, 1977; Finetti and Morelli, 1973; Giese and Morelli, 1975; Alpine Explosion Seismology Group, 1976; Colombi et al., 1977; Giese et al., 1977; Letz et al., 1977; Italian Explosion Seismology Group, 1978) as well as, when available, short period phase and group velocity dispersion results (Calcagnile and Panza, 1979; Calcagnile et al., 1979). Small to moderate fluctuations in crustal properties do not have a significant influence on the results of inversion for the upper mantle properties since we limit the shorter period cut-off of our phase velocity data to 25 sec. The lithosphere stripped of the crust ('lid') has been taken to be variable in thickness and shear wave velocity, as well as the asthenosphere ('channel') underneath. The parameterization of the structure is fully described in Fig. 7. Smaller incremental steps are meaningless compared to the resolving power of our data set (see Table 1a). In general the density, ρ , and the compressional wave velocity, α , have been kept fixed in all layers at popular values; however, data from body wave studies have been used whenever possible to assign the values of α . Since fundamental mode Rayleigh wave phase velocities in the period range we are dealing with depend almost completely on the shear wave structure of the upper mantle the inversion is not significantly affected by the choice we have made (e. g. Panza, 1981).

Table 1 Results of inversion for continental structure (Knopoff and Chang, 1977)

	Rayleigh waves		Love waves	
	c	U	c	U
rms error in data(km/s)	0.03	0.03"	0.03	0.03"
$\delta\beta_{LID}$ (km/sec)	0.144	0.086	0.116	0.101
$\delta\beta_{CH}$ (km/sec)	0.070	0.062	0.067	0.077
$\delta\beta_{SUB}$ (km/sec)	0.373	0.435	0.541	1.34
δh_{CR} (km)	4.55	2.46	4.90	3.47
δh_{LID} (km)	30.9	16.5	39.9	27.8
δh_{CH} (km)	49.2	52.6	75.2	142.2

Table 2b. Results of inversion for oceanic structure (Knopoff and Chang, 1977)

	Rayleigh waves		Love waves	
	c	U	c	U
rms error in data(km/s)	0.03	0.03"	0.03	0.03"
$\delta\beta_{LID}$ (km/sec)	0.127	0.063	0.144	0.130
$\delta\beta_{CH}$ (km/sec)	0.068	0.055	0.046	0.035
$\delta\beta_{SUB}$ (km/sec)	0.113	0.092	0.116	0.194
δh_{LID} (km)	11.9	6.4	37.0	24.6
δh_{CH} (km)	25.0	17.2	21.3	23.1

"For comparison with results of inversion of phase velocity data, multiply values in this column by the ratio σ_U / σ_c.

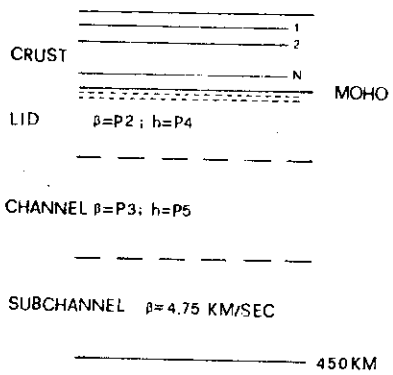

PARAMETER	RANGE
P2 [illegible]	4.05 (0.15) 4.80
P3 [illegible]	4.00 (0.1) 4.80
P4 [illegible]	15 (30) 135
P5 [illegible]	35 (70) 245

Figure 7
Parameterization used in the inversion. In some cases β = P1 in the lower crust or very thin layers were assumed underneath the Moho; numbers in parentheses indicate the parameter's increment.

Most of the results of this systematic inversion procedure are summarized in Fig. 8, which shows a schematic map of the lithosphere-asthenosphere system in the European area. As indicated in the legend, the various types of hatching signify regions of different thickness of the lower lithosphere (escluding the crust), i. e. the 'lid' above the asthenosphere 'channel'. The numbers in the upper line represent the average shear velocities (S_n) in the lower lithosphere, while the italic numbers (lower line) correspond to the shear velocities in the asthenosphere. For comparison the significant heat flow anomalies (Cermak and Hurtig, 1977) have also been included in the map. Only contours for heat flow values $Q \geq 80$ mW/m^2 and $Q \leq 40$ mW/m^2 are plotted in Fig. 8, so that the picture is not too confusing.

From the observations at very long periods the depth to the lower boundary of the asthenosphere could be determined to be 230 $\pm$ 40 km. This result indicates a relatively high degree of smoothness in the mantle structure at greater depth.

The map in Fig. 8 has been compared with another independent set of seismic data, namely a map depicting the depth to the minimum P wave velocity in the asthenosphere as constructed by Bisztricsany (1974) from first arrivals of shallow-focus earthquakes. The range of values for S waves presented in Fig. 8 is in good agreement with the P wave results of Bisztricsany (1974) and allows an estimate of the V_p/V_s ratio for the European area. It turns out to be of the order of 1.8 in the Western Mediterranean Basin, in South-Central France, the Western Alps, and the Tuscan Archipelago. The V_p/V_s ratio is about 1.7 in the 'Central European Rift System', in the Central Alps and in the North-Central Adriatic region.

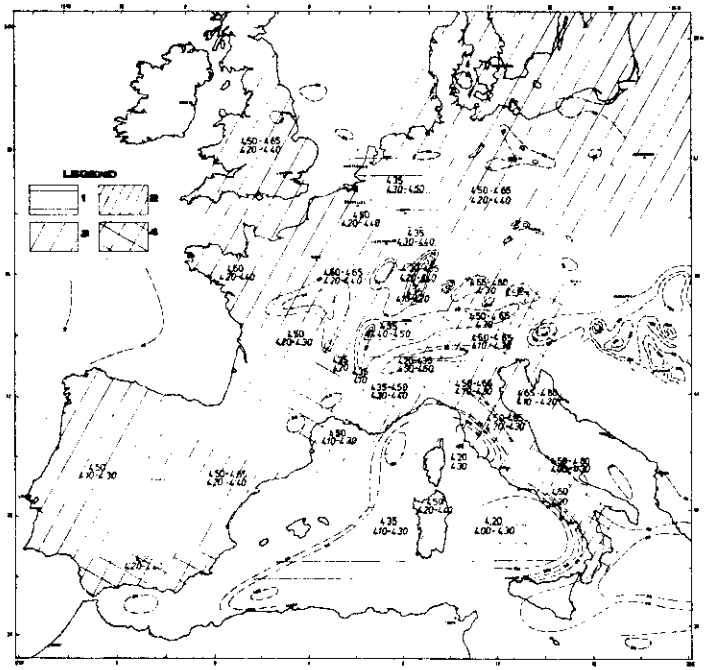

Figure 8

Schematic representation of upper mantle properties obtained by the 'hedgehog' inversion procedure. Different hatchings correspond to the maximum possible 'lid' thickness h (lower lithosphere, excluding the crust): $1 = h < 45$ km, $2 = h < 75$ km, $3 = h < 105$ km, $4 = h < 135$ km. Numbers in the upper line represent the sub-crustal S wave velocity (S_n) and italic numbers (lower line) give the range of S wave velocities (km/sec) in the asthenosphere. The broken isolines mark the surface heat flow anomalies (after Čermak and Hurtig, 1977) for $Q \leqslant 40$ mW/m^2 and $Q \geqslant 80$ mW/m^2.

If, for instance, we concentrate on the properties of the Italian region we can see that areas with thick lid (up to more than 100 km) are mainly associated to the Central and Southern Alps and the Po Basin (shear velocity 4.50-4.65 km/sec), while through a rather rapid transition the lid is less than 50 km thick in the North-Eastern Alps (shear velocity as low as 4.35 km/sec). Southern Adriatic and Southern Apennines have 'normal lid' (up to 75 km) characterized by shear velocity in the range 4.50-4.65 km/sec, channel shear velocity is about 4.3-4.4 km/sec. The Tuscan Archipelago and the Central Western Apennines have 'thin lid' (less than 15 km) and low shear velocity (4.05-4.35 km/sec), as well as the Balearic Basin and the Tyrrhenian Sea. The map of the lithosphere-asthenosphere system is shown in Fig. 9. In this map we see a maximum lithospheric depth under the Po River Valley, the Central and Southern Alps (as large as 130 km), while the minimum is reached in the Balearic and Tyrrhenian bathyal plains (less than 30 km). It must also be pointed out the very rapid transition in the lithospheric thickness from 130 km to 50 km going from the Alps to the Central European rift area. Smaller but significant lateral variations can be observed in the S-wave velocities of the lid and of the asthenospheric channel, which varies respectively from about 4.50-4.65 km/sec and 4.2-4.3 km/sec in correspondence of the Alps, to about 4.35-4.50 km/sec and 4.4-4.5 km/sec in correspondence of the Central European rift area.

To have a much more immediate insight on the lateral variations in the upper mantle and therefore on the depth range of interaction in the area we have sketched a few cross-sections, along the traces shown in Fig. 9. To avoid overcrowding, in the sections we have chosen

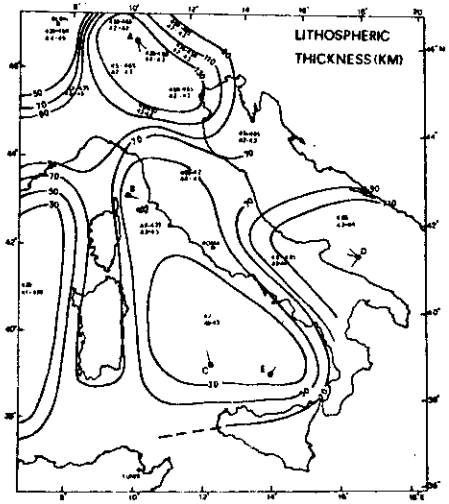

Figure 9
Lithospheric thickness in the Italian area.

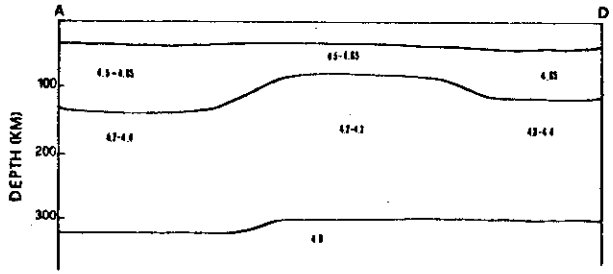

Figure 10
Cross section Central Alps-Southern Adriatic Sea (AD).

to draw crust-lid, lid-channel and channel-asthenosphere transitions as a line, representing the average value obtained from the inversion results; however, it must be kept in mind that the uncertainty in locating the three mentioned boundaries is of the order of about 5 km, 30 km and 70 km respectively (e. g. Panza, 1981).

Profile AD (Central Alps-Southern Adriatic Sea) crosses almost longitudinally the Adriatic Sea. From this cross-section (Fig. 10) we see a lithosphere-asthenosphere system with elastic properties rather typical for continental areas, while relevant thickness variations are detected. The lithosphere is relatively thick south of point A and north of point D, while in the central part it is thinned to about 80 km. The bottom of the channel is not well resolved by the data but seems to be at a depth of about 300 km.

Profile BD (Fig. 11) goes from the Tuscan Archipelago to the Southern Adriatic Sea. In the left part of the cross-section it is possible to see a thin veneer of high-velocity material at the top of the mantle overlying low-velocity material extending to a depth of the order of about 70-80 km. This soft layer is atop of higher velocity material extending to great depth. As we move south-eastward this character disappears and we reach again a typical continental lithosphere-asthenosphere system in the Southern Adriatic Sea.

In the profile CA (Central Alps-Southern Tyrrhenian Sea)(Fig. 12) we see the very large amount of lateral variation down to the bottom of the channel, which rises from about 300 km underneath the Central Alps at about 200 km in the bathyal plain. Also in the central part of this profile it must be noted below 60 km the presence of an anomalous zone with velocity in the range 4.4-4.6 km/sec, rather higher than usual

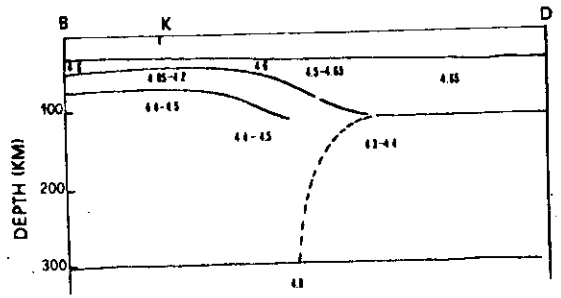

Figure 11
Cross section Tuscan Archipelago-Southern Adriatic Sea (BD), K is the cross point with cross section CA.

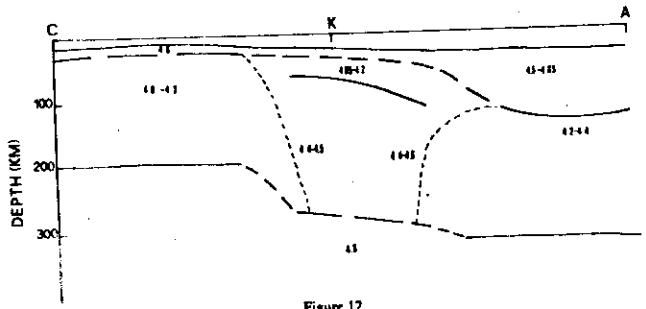

Figure 12
Cross section Central Alps-Southern Tyrrhenian Sea (CA).

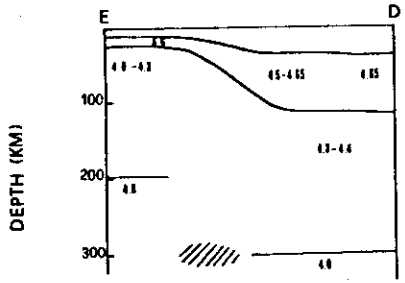

Figure 13
Cross section Southern Tyrrhenian Sea-Southern Adriatic Sea (ED), the hatched area indicates the location of intermediate earthquakes (e.g. PANZA, 1978).

channel values, underlying sub-Moho low-velocity material (shear velocity around 4.05-4.2 km/sec). The last cross-section, Southern Tyrrhenian-Southern Adriatic Sea (Fig. 13) shows the rapid transition from typical continental lithosphere in the Southern Adriatic to the oceanic-type upper mantle structure under the Tyrrhenian Sea.

In Figs. 11 and 12 (short dashes) a possible interpretation of the S-wave velocity distribution is given. The relatively high velocities detected in the depth range 100-300 km, in correspondence of Central Italy, can be interpreted as indicators of the presence of 'lithospheric roots' similar to the ones detected in the Western Alps by Panza and Mueller (1978), and probably associated with the continent-continent collision started in the Eocene. On the other side the very low velocity material present just below the Moho can be interpreted as the result of rifting processes subsequent to the collision.

The results described up to now combined with more recent measurements allow the construction of a map of lithosphere properties for broader area (Fig. 14), which contributes to progress in the understanding of the large scale tectonic processes.

5. Lithospheric model

The lithospheric thickness, which can be determined with an uncertainty of about 30 km (Panza, 1981), shows two maxima one north of the Po valley and the other in the vicinity of Greece where it reaches 130 km, while in the same regions the lid shear-wave velocity is characterized by values as high as 4.50-4.70 km s^{-1}. Under the southern Adriatic Sea the lithosphere is 110 km thick with a lid shear-wave velocity of 4.50-4.65 km s^{-1}. In the north-central Apennines the litho-

sphere is relatively thin, with a thickness of about 70 km, and possibly of low rigidity, since the lid shear-wave velocity has values of 4.05-4.20 km s^{-1}. In the Tyrrhenian Sea there is a minimum lithospheric thickness of 30 km and a lid shear-wave velocity of 4.20 km s^{-1}. Under the Calabrian and Hellenic Arcs the map shows strong lithospheric gradients while beneath almost all the Ionian Sea region the lithosphere is about 90 km thick with a velocity of 4.40-4.60 km/s in the upper mantle.

From the model in Fig. 14 we may infer that some of the proposed active boundaries of the interacting Mediterranean microplates (e. g. see Lort, 1971) are also delineated by strong gradients of lithospheric thickness.

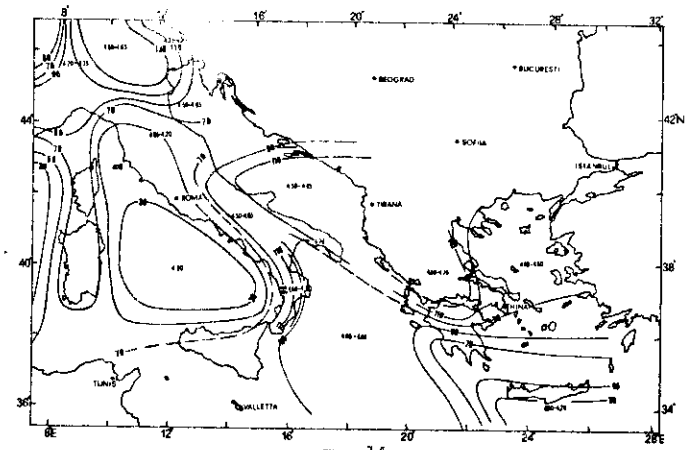

Figure 14
Synoptic representation of the lithospheric thickness and of the lid velocity.

6. Earthquakes distribution

The analysis of the epicentral distribution of shallow shocks including historical ones for the Italian area from 1000 to 1980 (Iaccarino, 1968; Scarpa et al., 1982) and of the earthquakes which occurred in the Balcanic and Aegean region from 1901 to 1979 (Karnik, 1969; Comninakis and Papazachos, 1978; Basili et al., 1979) shows that the Mediterranean area is characterized by a particular pattern of seismic activity. It is very difficult to correlate such seismic activity with the presently available lithospheric model. However, if a high-pass filter, for magnitude or intensity, is applied to the available data the correlation shown in Fig. 15 is obtained. In the figure, only the shallow events (open circles) with $M \geq 6.5$ or $I \geq X$ are represented together with the lithospheric properties.

In Fig. 15 the directions of the P and T axes derived from the few available fault-plane solutions of earthquakes with $M \geq 6.5$ (McKenzie, 1972; Riuscetti and Shick, 1975; Ebblin, 1980; Gasparini et al., 1980) are shown by arrows.

It can be pointed out that the strongest events are concentrated along belts characterized not only by a strong gradient in lithospheric thickness, but also by a comparatively high rigidity in the lid. As examples we can quote the southern Apennines, the Calabrian and the Hellenic Arcs. On the other hand strong seismic events are practically absent in areas, like central Italy and south of Crete, where the thinning of the lithosphere is associated with relatively low values of shear-wave velocity in the upper mantle. The absence of seismicity around the Corsica-Sardinia massif is not contradicting our model since the transition of this block to the Balearic and Tyrrhenian basins can

be considered of Atlantic type (Scandone, 1979). In more detail it can be observed that in Italy, as already noted by Panza et al. (1981), there is a concentration of strong shocks in the eastern and southern Alps, in the southern part of the Calabrian Arc and on the western side of the south-central Apennines bounded in the north by the Anzio-Ancona line and by 40°N latitude to the south. On the other hand a lack of shocks with $M \geq 6.5$ is observed in the western Alps, in the north-central Apennines up to the Anzio-Ancona line, in the northern part of the Calabrian Arc and in northern Sicily. It must be remarked that the Calabrian Arc is the only Italian region characterized by earthquakes with $M \geq 7$. Furthermore, in the southern Apennines the estimated mean return period for shocks with $M \geq 6.5$ is 30-50 years, while the eastern Alps are characterized by a much longer mean return period.

To the east, the earthquakes with $M \geq 6.5$ have the smallest mean return periods over the total area considered, and are concentrated along the Hellenic Arc and around the Greek mainland, along belts characterized by rapid lateral variations in lithospheric thickness.

Strong seismic activity is not recorded south of Crete, where the upper mantle has low rigidity values (S-wave velocity = 4.00-4.20 km s^{-1}), and over the whole Ionian Sea region, which behaves as the passive (Atlantic-type) continental margin of Africa (Channel et al., 1979), bounded to the northwest and northeast by two zones of intermediate to deep seismic zones (see Fig. 15) of the Calabrian and Hellenic Arcs (e. g. Caputo et al., 1970; Papazachos and Comninakis, 1971; Panza, 1979; Gasparini et al., 1982).

CAPTION

Fig. 15. Synoptic representation of lithospheric properties and distribution in space of shallow seismic events with $M \geq 6.5$. The size of the circles, representing epicenters, is proportional to focal volume. The space distribution of intermediate and deep focus earthquakes is schematized by thick dashed lines. The few available fault-plane solutions are schematized by means of arrows.

Fig. 15

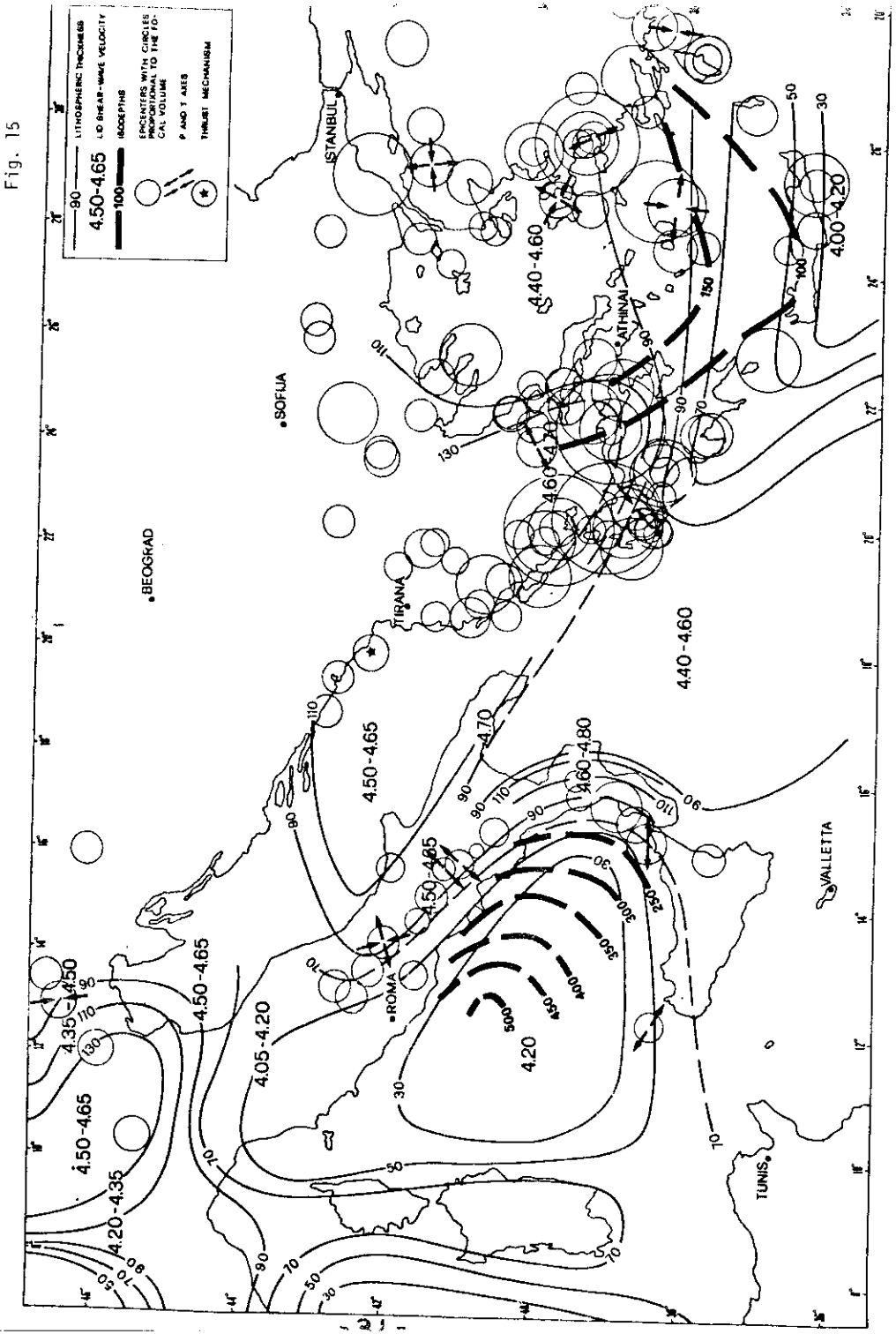

Conclusions

The attempt to correlate the main seismic activity with lithospheric properties indicates that the largest shocks tend to occur along belts where lid rigidity values very close to those of the stable areas are associated with very rapid changes in the lithospheric thickness. This is the case for northern and southern Italy, the Calabrian and Hellenic Arcs. On the contrary, the considered seismicity seems to be totally absent in areas, namely the central Apennines and south of Crete, were significant reduction of lid rigidity is observed.

The lack of strong shocks in the Corsica-Sardinia area can be accounted for by considering that the Corsica-Sardinia massif, which has behaved as a passive block at least from Late Miocene-Early Pliocene (Scandone, 1979), is an Atlantic-type transition to the Tyrrhenian and the Balearic basins.

Thus, the investigation of the structure of the Upper Mantle in the Mediterranean area allows a physical understanding of the occurrence in space of the main shocks. In other words, the active belts can be defined not only on the basis of historical seismic records, but also on the basis of structural properties.

If the proposed model is accepted, any area within these belts may be affected by an earthquake with magnitude greater or equal to 6.5. Conversely, according to this model, for the areas with a "soft" lid the occurrence of a shock with $M \geq 6.5$ seems to be highly unlikely. The importance of such findings for a physical understanding of earthquake occurrence makes a more detailed investigation of the structural properties necessary, mainly in those part of the belts which have not yet experienced a strong earthquake.

References

Aki, K., 1972. Earthquake mechanism.
Tectonophysics, 13, 423-446.

Alpine Explosion Seismology Group, 1976. A lithospheric seismic profile along the axis of the Alps, 1975. I: First results.
Pure appl. Geophys., 114, 1109-1130.

Anderson, D. L., 1964. Universal dispersion tables, I, Love waves across oceans and continents on a spherical earth.
Bull. Seism. Soc. Am., 54, 681-726.

Anderson, D. L. and Harkrider, D. G., 1968. Universal dispersion tables, II, Variational parameters for amplitudes, phase velocity and group velocity for first four Love modes for an oceanic and continental earth model.
Bull. Seism. Soc. Am., 58, 1407-1499.

Basili, M., [illegible], F., Cipolliini, A., De Marco, R., De Simoni, B., Giacalone, P., Giorgetti, E., Marson, P., Sabetta, F., Sanò, T. and Scandone, P., 1979. Il terremoto del Montenegro del 15 aprile 1979.
Consiglio Superiore dei Lavori Pubblici, Servizio Sismico, 1-66.

Berry, M. J. and Knopoff, L., 1967. Structure of the upper mantle under the Western Mediterranean basin.
J. Geophys. Res., 72, 3613-3626.

Biswas, N. N., 1971. The upper mantle structure of the United States from dispersion of surface waves.
Ph.D. Thesis (IGPP, UCLA, Los Angeles, 1971).

Biswas, N. N. and Knopoff, L., 1974. Structure of the upper mantle under the United States from the dispersion of Rayleigh waves.
Geophys. J. R. astr. Soc., 36, 515-539.

Bisztricsany, E., 1974. The depth of the LVL in Europe and in some adjacent regions.
Geofizikai Közlemenyek 22, 61-63.

Calcagnile, G. and Panza, G. F., 1974. Vertical and SV components of Sa.
Geophys. J. R. astr. Soc., 38, 317-325.

Calcagnile, G., D'Ingeo, F. and Panza, G. F., 1979. On the properties of the lithosphere in South-Eastern Europe as deduced from Rayleigh wave group velocity data.
VI Europ. Geophys. Soc., Vienna.

Calcagnile, G. and Panza, G. F., 1979. Crustal and upper mantle structure beneath the Apennines region as inferred from the study of Rayleigh waves.
J. Geophys., 45, 319-327.

Caputo, M., Panza, G. F. and Postpischl, D., 1970. Deep structure of the Mediterranean basin.
J. Geophys. Res., 75, 4919-4923.

Channel, J. E. T., D'Argenio, B. and Horvat, F., 1979. Adria, the African promontory, in Mesozoic Mediterranean paleogeography.
Earth Sci. Rev., 15, 213-292.

Colombi, B., Guerra, I. and Scarascia, S., 1977. Crustal structure along two seismic refraction lines in the Northern Apennines (Line 16 and 2).
Boll. Geof. Teor. Appl., 19, 214-224.

Comninakis, P. E. and Papazachos, B. C., 1978. A catalogue of earthquakes in the Mediterranean and surrounding area for the period 1901-1975.
University of Thessaloniki, Geophysical Laboratory. Publ. No. 5, 1-146.

Dziewonski, A. M. and Hales, A. L., 1972. Numerical analysis of dispersed seismic waves, in Methods in Computational Physics (ed. by B. A. Bolt).
Vol. 11, Academic Press, New York, 39-85.

Ebblin, C., 1980. Fault-plane solutions and hypocentral distribution of some 1977 Friuli aftershocks.
Geophys. J., 62, 97-112.

Finetti, I. and Morelli, C., 1973. Geophysical exploration of the Mediterranean Sea.
Boll. Geof. Teor. Appl., 15, 263-340.

Gasparini, C., Iannaccone, G. and Scarpa, R., 1980. On the focal mechanisms of Italian earthquakes.
Rock Mech. 9, 85-91.

Gasparini, C., Iannaccone, G., Scandone, P. and Scarpa, R., 1982. Seismotectonics of the Calabrian Arc.
Tectonophysics, 84, 267-289.

Hildebrand, F. B., 1956. Introduction to numerical analysis.
McGraw Hill Book Company, New York.

Giese, P. and Morelli, C., 1975. Crustal structure in Italy.
Quaderni de "La Ricerca Scientifica", CNR, Roma, 90, 453-489.

Giese, P., Morelli, C. and Nicolich, R., 1977. Review on the crustal structure of the Ligurian Sea and adjacent area.
Boll. Geof. Teor. Appl., 19, 253-258.

Iaccarino, E., 1968. Attività sismica in Italia dal 1893 al 1965.
Comitato Nazionale Energia Nucleare, Roma, 1-70.

Italian Explosion Seismology Group, 1978. Preliminary interpretation of the profile HD across the Eastern Alps.
Boll. Geof. Teor. Appl., 20, 287-302.

James, D. E. and Linde, A. T., 1971. A source of major error in the digital analysis of world wide standard station seismograms.
Bull. Seism. Soc. Am., 61, 723-728.

Karnik, V., 1969. Seismicity of the European area. Part I.
Reidel, Dordrecht, Netherlands, 1-364.

Keilis-Borok, V. I. and Yanovskaya, T. B., 1967. Inverse problems in seismology.
(Structural Review), Geophys. J. R. astr. Soc., 56, 223-234.

Knopoff, L., 1972. Observation and inversion of surface-wave dispersion.
Tecto[illegible]s, 13, 497-519.

Knopoff, L., Mueller, S. and Pilant, W. L., 1966. Structure of the crust and upper mantle in the Alps from the phase velocity of Rayleigh waves.
Bull. Seism. Soc. Am., 56, 1009-1044.

Knopoff, L., Schwab, F. and Kausel, E., 1973. Interpretation of Lg.
Geophys. J. R. astr. Soc., 36, 737-742.

Landsman, M., Dziewonski, A. and Satō, Y., 1969. Recent improvements in the analysis of surface wave observations.
Geophys. J. R. astr. Soc., 17, 369-403.

Letz, H., Reichert, C. and Wigger, P., 1977. Results of two seismic refraction lines in the Northern Apennines (Lines 1 and 3).
Boll. Geof. Teor. Appl., 19, 225-232.

Lort, J. K., 1971. The tectonics of the Eastern Mediterranean. A Geophysical Review. Rev. Geophys., 9, 189-216.

McEvilly, T. V., 1964. Central U. S. crust-upper mantle structure from Love and Rayleigh wave phase velocity inversion.
Bull. Seism. Soc. Am., 54, 1997-2015.

McKenzie, D., 1972. Active tectonics of the Mediterranean region.
Geophys. J. R. astr. Soc., 30, 109-185.

Morelli, C., Carrozzo, M. T., Ceccherini, P., Finetti, I., Gantar, C., Pisani, M. and Schmidt di Friedberg, P., 1969. Regional geophysical study of the Adriatic Sea.
Boll. Geof. Teor. Appl., 11, 3-48.

Morelli, C. and Giese, P., 1977. Seismic refraction measurements between the Northern Apennines and Corsica, 1974.
Boll. Geof. Teor. Appl., 19, 201-206.

Morelli, C., Giese, P., Cassinis, R., Colombi, B., Guerra, I., Luongo, G., Scarascia, S. and Schütte, K. G., 1975. Crustal structure of Southern Italy. A seismic refraction profile between Puglia-Calabria-Sicily.
Boll. Geof. Teor. Appl., 17, 183-210.

Morelli, C., Giese, P., Hirn, A., Colombi, B., Eva, C., Guerra, I., Letz, H., Nicolich, R., Reichert, C. and Wigger, P., 1976. Investigations of crustal and upper mantle structure of the Northern Apennines and Corsica.
International Symposium on the Structural History of the Mediterranean Basins, Split (Edition Technip., Paris), 281-286.

Nolet, G., 1975. Higher Rayleigh modes in Western Europe.
Geophys. Res. Letters, 2, 60-62.

Nolet, G., 1977. The upper mantle under Western Europe inferred from the dispersion of Rayleigh modes.
J. Geophys., 43, 265.

Nolet, G. and Panza, G. F., 1976. Array analysis of seismic surface waves: limits and possibilities.
Pure and Appl. Geophys., 114, 773.

Ormsby, J. F. A., 1961. Design of numerical filters with application to missile data processing.
J. Assoc. Comp., March 8, 440-466.

Panza, G. F., 1974. Focal-mechanism determination from multimode Rayleigh wave response.
Phys. Earth and Plan. Int., 8, 345-351.

Panza, G. F., 1979. The crust and upper mantle in Southern Italy from geophysical data.
Riv. Ital. Geofis., Spec. Issue, 17-22.

Panza, G. F., 1981. The resolving power of seismic surface waves, in: R. Cassinis (Editor). The Solution of the Layers Problem in Geophysical Interpretations.
Plenum, New York, 39-77.

Panza, G. F. and Calcagnile, G., 1974a. Comparison of the multimode surface wave response in structures with and without a low-velocity channel (Part I: dip-slip sources in a vertical fault plane).
Pure Appl. Geophys., 112, 583-596.

Panza, G. F. and Calcagnile, G., 1974b. Comparison of the multimode surface wave response in structures with and without a low-velocity channel (Part II: dip-slip sources).
Pure Appl. Geophys., 112, 1031-1043.

Panza, G. F. and Calcagnile, G., 1975. Comparison of the multimode surface wave response in structures with and without a low-velocity channel (Part III: strike-slip sources).
Pure Appl. Geophys. 113, 661-671.

Panza G. F., Calcagnile, G., Scandone, P. and Mueller, S., 1980. La struttura profonda dell'area Mediterranea.
Le Scienze, 24, 60-69.

Panza, G. F. and Mueller, S., 1978. The plate boundary between Eurasia and Africa in the Alpine area.
Mem. Soc. Geol., 33, 43-50.

Panza, G. F., Mueller, S. and Knopoff, L., 1975. The upper mantle structure of the Southern Alpine foreland.
Rapp. Comm. Int. Mer. Medit., 23, 50.

Panza, G. F., Scandone, P. and Scarpa, R., 1981. Sul comportamento dinamico della litosfera nell'area italiana.
Rend. Soc. Geol. It., 4, 571-572.

Panza, G. F., Schwab, F. and Knopoff, L., 1973. Multimode surface waves for selected focal mechanisms. I. Dip-slip sources on a vertical fault plane.
Geophys. J. R. astr. Soc., 34, 265-278.

Panza, G. F., Schwab, F. and Knopoff, L., 1975a. Multimode surface waves for selected focal mechanisms. II. Dip-slip sources.
Geophys. J. R. astr. Soc., 42, 931-943.

Panza, G. F., Schwab, F. and Knopoff, L., 1975b. Multimode surface waves for selected focal mechanisms. III. Strike-slip sources.
Geophys. J. R. astr. Soc., 42, 945-955.

Papazachos, B. C. and Comninakis, P. E., 1971. Geophysical and tectonic features of the Aegean arc.
J. Geophys. Res., 76, 8517-8533.

Pilant, W. L. and Knopoff, L., 1964. Observation of multiple seismic events.
Bull. Seism. Soc. Am., 54, 19-39.

Reichenbach, H. and Mueller, S., 1974. Ein Krusten-Mantel-Modell für das Riftsystem um den Rheingraben, abgeleitet aus der Dispersion von Rayleigh-Wellen, Approaches to Taphrogenesis, ICG Scientific Rept., 8, 348-354 (Schweizerbart-Verlag Stuttgart).

Riuscetti, M. and Schick, R., 1975. Earthquakes and tectonics in Southern Italy.
Boll. Geof. Teor. Appl., 17, 59-78.

Satô, Y., 1955. Analysis of dispersed surface waves by means of Fourier transform. I.
Bull. Earthquake Res. Inst. (Tokyo Univ.), 33, 33-50.

Satô, Y., 1956. Analysis of dispersed surface waves by means of Fourier transform. III: Analysis of practical seismogram of South Atlantic earthquake.
Bull. Earthquake Res. Inst. (Tokyo Univ.), 34, 131-138.

Scandone, P., 1979. Origin of the Tyrrhenian Sea and the Calabrian Arc.
Boll. Soc. Geol. It., 98, 27-34.

Scarpa, R., Ciaranfi, N., Cuscito, M., Guerra, I., Guida, M., Iaccarino, G., Iannaccone, G., Panza, G. F., Pescatore, M. T., Pieri, P., Rapisardi, L., Ricchetti, G., Scandone, P., Sgrosso, I., Torre, M., Tortorici, L. and Turco, E., 1982. Elementi sismotettonici dell'Appennino meridionale.
Boll. Soc. Geol. It., in press.

Schwab, F., Kausel, E. and Knopoff, L., 1973. Interpretation of Sa for a shield structure.
Geophys. J. R. astr. Soc., 36, 737-742.

Seidl, D. and Mueller, S., 1977. Seismische Oberflächenwellen (Seismic Surface Waves).
J. Geophys., 42, 283-328.

Sprecher, Ch., 1976. Die Struktur des oberen Erdmantels in Zentraleuropa aus Dispersionsmessungen an Rayleigh-Wellen.
Dissertation ETH Zürich, No. 5864, 156 p.

Toksöz, M. N. and Anderson, D. L., 1966. Phase velocities of long-period surface waves and structure of the upper mantle. I. Great-circle Love and Rayleigh wave data.
J. Geophys. Res., 71, 1649-1658.

Toksöz, M. N. and Ben Menahem, A., 1963. Velocities of mantle Love and Rayleigh waves over multiple paths.
Bull. Seism. Soc. Am., 53, 741-764.

Tsai, Y. B. and Aki, K., 1970. Precise focal-depth determination from amplitude spectra of surface waves.
J. Geophys. Res., 75, 5729-5743.

Tsai, Y. B. and Aki, K., 1971. Amplitude spectra of surface waves from small earthquakes and underground nuclear explosion.
J. Geophys. Res., 76, 3940-3952.